VERTICAL PROFILES OF THE STRUCTURE PARAMETER OF TEMPERATURE IN THE STABLE, NOCTURNAL BOUNDARY LAYER

J. W. M. CUIJPERS and W. KOHSIEK
Royal Netherlands Meteorological Institute, De Bilt, The Netherlands

(Received in final form 2 September, 1988)

Abstract. Vertical profiles of the structure parameter of temperature C_T^2 in the stable, nocturnal boundary layer (NBL) have been obtained with the analytic models described by Nieuwstadt (1984, 1985) and Sorbjan (1986) and the numerical model of Duynkerke and Driedonks (1987). These theoretical profiles are compared with observed profiles from the meteorological mast at Cabauw, The Netherlands. From the observations, it is found that C_T^2 is large in the surface layer and small at the top of the NBL. Observations during nights with moderate geostrophic winds or during the first few hours of nights with a high geostrophic wind show a continuous decrease of C_T^2 from the surface layer to the top of the NBL. Observations made later on nights with a high geostrophic wind show the development of a maximum of C_T^2 at about three quarters of the NBL. From the comparison with the models, we conclude that the observed profiles are most satisfactorily described by the model of Duynkerke and Driedonks.

1. Introduction

The temperature structure parameter, which is a measure of temperature fluctuations in a turbulent atmosphere, is of interest for several reasons. It can be used as a diagnostic tool, such as sensing the height of the turbulent layer with an acoustic radar, or inferring the surface heat flux either acoustically (Coulter and Wesely, 1980) or from *in-situ* observations of C_T^2 (Champagne *et al.*, 1977). It may also be applied to study the influence of atmospheric turbulence on the propagation of electromagnetic and acoustic waves, such as the effect on stellar imaging (Coulman, 1985) and on satellite-earth communication links (Herben, 1983). The atmospheric phenomenon, known as scintillation, is exploited in so-called scintillometers, instruments by which line-averaged surface fluxes of heat, moisture and momentum may be measured by means of the influence of the atmosphere on the propagation of a usually horizontal beam of light or radiation (Hill and Ochs, 1983; Ochs and Hill, 1985). In this paper we present observations of vertical profiles of the structure parameter of temperature obtained from the meteorological mast at Cabauw, The Netherlands, during clear nights and we compare them with the analytic models described by Nieuwstadt (1984, 1985) and Sorbjan (1986) and the numerical model of Duynkerke and Driedonks (1987).

During clear nights, the atmospheric boundary layer usually is stably stratified due to radiative cooling at the land surface. Vertical motion is restricted and

Boundary-Layer Meteorology **47**: 111–129, 1989.
© 1989 *Kluwer Academic Publishers. Printed in the Netherlands.*

turbulence is weak. Moreover the dynamics of the stable boundary layer may be influenced by more processes than continuous turbulence alone. Internal gravity waves (Finnigan and Einaudi, 1981), longwave atmospheric radiation (Garratt and Brost, 1981) and intermittent turbulence (Kondo *et al.*, 1978) may be important and can complicate the structure of the stable boundary layer. We selected nights that are characterized by continuous turbulence and that did not show the presence of significant gravity wave activity.

Observations of turbulence variables in general and of the structure parameter of temperature in particular in a stable boundary layer are not as abundant as in convective circumstances, e.g., Wyngaard and LeMone (1980) and Fairall (1987). Except for the data shown by Caughey *et al.* (1979), which are based on runs during early evening, we are not aware of other observations of vertical profiles of the temperature structure parameter.

2. Observations

Between September 1977 and February 1979 and in August 1983, experiments were conducted on the meteorological mast at Cabauw during clear stable nights (Nieuwstadt, 1984). The observations were begun about 2–3 hours after sunset to avoid the transition period during which turbulence is dominated by non-stationary effects.

The mast at Cabauw is 213 m high and the surrounding terrain is flat and homogeneous on a scale of approximately 20 km (Monna and van der Vliet, 1987). At height intervals of 20 m, booms are installed in three directions. The instruments and measuring heights used during the experiments are given in Table I.

Turbulent wind fluctuations were measured with a trivane (Wieringa, 1967 and 1972). A trivane consists of a propeller attached to one end of a rod, that can turn around two axes and is kept in the wind direction by means of an annular fin at the other end. The azimuth and elevation angle of the rod are determined by potentiometers.

Turbulent temperature fluctuations were measured from September 1977 to February 1979 with a pair of 100 μm copper-constantan thermocouples, mounted

TABLE I

The experimental set-up during nocturnal boundary-layer experiments.

Parameter	Instrument	Measuring height (m)
Turbulence	Trivane, fast thermocouple	20, 40, 80, 120, 160, 200
Wind speed	Cup anemometer	10, 20, 40, 80, 120, 160, 200
Wind direction	Wind vane	20, 40, 80, 120, 160, 200
Temperature	Ventilated thermocouples	10, 20, 40, 80, 120, 160, 200
Boundary-layer height	Acoustic sounder	

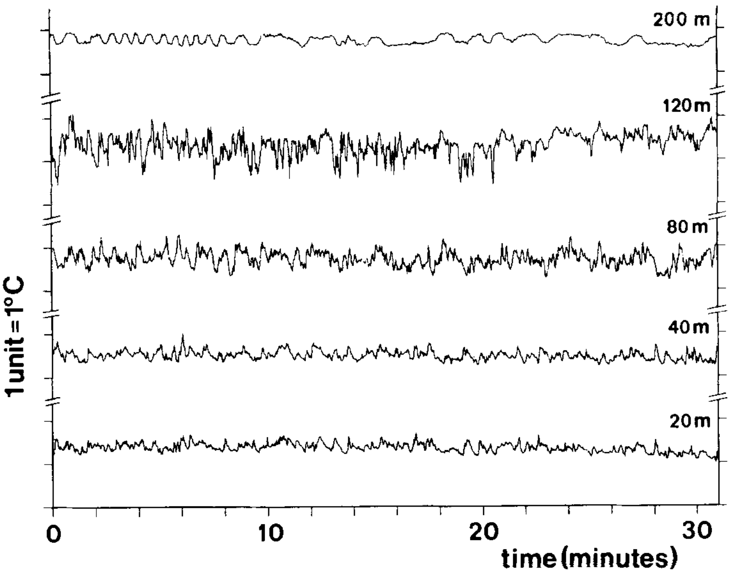

Fig. 1. Temperature traces at several heights as a function of time, 20 February, 1978, 22:00–22:30 GMT. Temp in °C. (Geostrophic wind ≈ 11 m/s).

on both sides of the trivane (1 m apart). In August 1983, only one fast-response thermocouple was used. In Figure 1, examples of traces of temperature as a function of time are shown for different heights. Observed vertical profiles of half-hourly mean potential temperature, wind speed and wind direction for the same period as in Figure 1 are shown in Figure 2.

All turbulent data were sampled with a frequency of 5 Hz and stored on magnetic tape. Variances and covariances of the velocity and temperature fluctuations were calculated over a time period of 30 min after removing a linear trend from the time series. By this procedure, only fluctuations with time scales ≤15 min contribute to the (co)variances. The average wind speed, wind direction and temperature were determined over concurrent 30 min periods.

Because only situations with continuous turbulence will be considered, half-hour runs with a geostrophic wind speed $\geq 5\ \mathrm{m\ s^{-1}}$ were selected. In such cases, the wind shear is large enough to maintain a continuous turbulent state. By using only observations for which the vertical velocity variance decreases continuously with height, we excluded boundary layers which are dominated by gravity waves (Driedonks and de Baas, 1983). Finally, we demanded that $h/L \geq 1$ (stability criterion), where h is the boundary-layer height determined with an acoustic sounder and L the Monin–Obukhov length. After this selection procedure, 62 half-hour runs remained for analysis of the structure parameter of temperature (Table II).

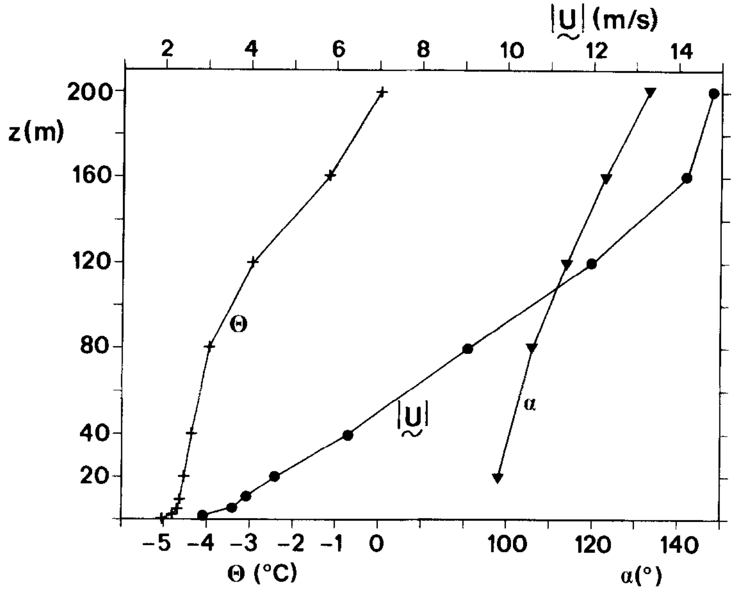

Fig. 2. Measured vertical profiles of half-hourly mean potential temperature Θ, wind speed |U| and wind direction α at Cabauw, 20 February, 1978, 22:00–22:30 GMT. The height of the boundary layer was 150 m.

TABLE II

Half-hour runs used to determine structure parameter of temperature.

Date	Observation period begin (GMT)	end (GMT)	Number of half-hour runs
20/21 Feb 1978	19:00	06:00	17
19 May 1978	00:00	03:30	8
29/30 May 1978	23:00	01:00	4
31 May/1 Jun 1978	22:30	02:00	8
26 Sep 1978	01:00	04:00	7
9 Feb 1979	04:30	08:00	7
30/31 Aug 1983	20:00	01:30	11

3. The Structure Parameter of Temperature

The temperature structure function D_T is defined as the mean-square temperature difference between two microthermal probes:

$$D_T \equiv \overline{[T(x) - T(x+R)]^2}\,, \tag{1}$$

where $T(x)$ is the temperature at position x, and $T(x+R)$ that at $x+R$. The overbar indicates an ensemble average, which in practice is replaced by time averaging. On the assumptions of an inertial subrange and local isotropy and homogeneity, the relation between D_T and the structure parameter of temperature is given by (Tatarski, 1961):

$$C_T^2 = \frac{\overline{[T(x) - T(x+R)]^2}}{|R|^{2/3}} = D_T(R)R^{-2/3} . \tag{2}$$

C_T^2 is independent of R if the separation $|R|$ is within the inertial subrange.

C_T^2 can be measured with two temperature sensors separated by a distance R, or with one sensor using measurements at different instants of time. In the latter case, $T(x, t+\tau)$ is put equal to $T(x+R, t)$ with $R = U\tau$; U is the mean wind speed and τ is the time delay.

The spectrum for temperature fluctuations is given by (Hinze, 1975):

$$F_T(k) = 0.25 C_T^2 k^{-5/3} . \tag{3}$$

In this study, we used (3) to infer the temperature structure parameter C_T^2 from observed spectra. The error in the values of C_T^2 is estimated at 20%. Comparing (3) with Corrsin's inertial subrange form for temperature (Corrsin, 1951):

$$F_T(k) = 0.8 N\epsilon^{-1/3} k^{-5/3} , \tag{4}$$

leads to:

$$C_T^2 = 3.2 N\epsilon^{-1/3} , \tag{5}$$

where ϵ is the dissipation of turbulent kinetic energy and N is the dissipation of temperature variance. So, a fourth way to determine the structure parameter C_T^2 is by these molecular destruction terms. This method will be used in the models, to be described in the next section.

4. The Vertical Profile of the Temperature Structure Parameter: Models

Several models have been developed to describe the nocturnal boundary layer. The model of Nieuwstadt (1984, 1985) is a steady-state second-order closure model to study the vertical structure of the stable boundary layer. In Section 4a we shall discuss this model and focus on the vertical profile of the structure parameter C_T^2. Another approach is offered in Section 4b: once the vertical profiles of the Reynolds stress τ and the turbulent heat flux $\overline{w'\theta'}$ have been determined, one can determine the vertical profile of C_T^2 using similarity theory. Thirdly, Duynkerke and Driedonks (1987) developed a multilevel ensemble-averaged E–1 model to study the cloud-topped atmospheric boundary layer. With this model, the structure parameter C_T^2 can be calculated as a function of height. A discussion of this model will be given in Section 4c.

4a. The Model of Nieuwstadt

To solve the equations that describe the evolution of the mean temperature Θ and the mean wind speed vector $\mathbf{U} = (U, V)$ in a horizontally homogeneous boundary layer, Nieuwstadt (1985) added as a closure hypothesis that the gradient Richardson number, Ri, and the flux Richardson number, Ri_f, are constant:

$$\mathrm{Ri} \equiv \frac{g}{T}\frac{\partial \Theta}{\partial z} \Big/ \left|\frac{\partial \mathbf{U}}{\partial z}\right|^2 = \text{constant}, \tag{6a}$$

$$\mathrm{Ri}_f \equiv -\frac{g}{T}\overline{w'\theta'} \Big/ \left(\boldsymbol{\tau}\cdot\frac{\partial \mathbf{U}}{\partial z}\right) = \text{constant}, \tag{6b}$$

where $\boldsymbol{\tau}$ is given by: $\boldsymbol{\tau} = [\overline{(-u'w')}, \overline{(-v'w')}]$. It is further assumed that there is a stationary, stable boundary layer.

With this model, the production terms of turbulent kinetic energy and temperature variance become:

$$-\overline{u'w'}\frac{\partial U}{\partial z} - \overline{v'w'}\frac{\partial V}{\partial z} = \frac{1}{k\mathrm{Ri}_f}\frac{u_*^3}{L}(1 - z/h), \tag{7a}$$

$$-\overline{w'\theta'}\frac{\partial \Theta}{\partial z} = -\frac{\mathrm{Ri}}{k\mathrm{Ri}_f}\frac{T_*}{L}\overline{w'\theta'_0}, \tag{7b}$$

where u_* is the friction velocity and $\overline{w'\theta'_0}$ is the surface heat flux. The temperature scale T_* and the Obukhov-length L are defined by:

$$T_* = -\overline{w'\theta'_0}/u_*, \tag{8a}$$

$$L = -u_*^3/(kg/T\overline{w'\theta'_0}), \tag{8b}$$

with k the von Karman constant. With (7), the molecular destruction terms ϵ and N in Equation (5) can be found from the complete turbulent kinetic energy and temperature variance budgets (Businger, 1982) and neglecting the time variation, advection and flux divergence terms (Brost and Wyngaard, 1978):

$$\frac{kh\epsilon}{u_*^3} = \frac{1 - \mathrm{Ri}_f}{\mathrm{Ri}_f}\frac{h}{L}(1 - z/h), \tag{9a}$$

$$\frac{khN}{T_*^2 u_*} = \frac{\mathrm{Ri}}{\mathrm{Ri}_f^2}\frac{h}{L}. \tag{9b}$$

Note that the temperature dissipation N is independent of height.

Now we can use Equation (5) to find the vertical profile of the structure parameter of temperature:

$$\frac{C_T^2 (kh)^{2/3}}{T_*^2} = 3.2\frac{\mathrm{Ri}}{\mathrm{Ri}_f^{5/3}(1 - \mathrm{Ri}_f)^{1/3}}\left(\frac{h}{L}\right)^{2/3}(1 - z/h)^{-1/3}. \tag{10}$$

It follows that towards the surface, C_T^2 approaches a constant value. This value and consequently the whole profile is a function of the stability parameter h/L.

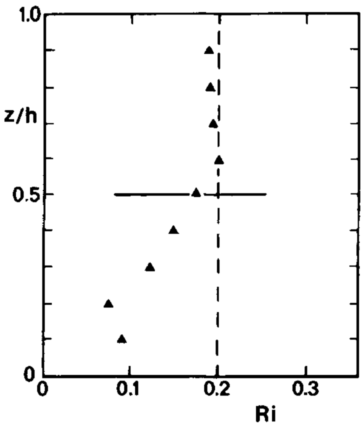

Fig. 3. The Richardson number as a function of non-dimensional height. Each point indicates the average of all observations within a given height interval. The horizontal bar indicates the standard deviation of the data (from Nieuwstadt, 1985).

The values for Ri and Ri_f are taken equal to 0.2, which seems to be a reasonable assumption for a major part of the boundary layer (Figure 3). Equation (10) also predicts that C_T^2 increases with height. The profile of C_T^2 is determined by the profile of ϵ solely, because, as noted above, N is constant with height. Figure 4 (thin lines) shows the calculated profiles of the dimensionless structure parameter $\mathrm{CTN} = (C_T^2(kh)^{2/3}/T_*^2)$ for different values of the stability parameter h/L. Note that for $z/h \rightarrow 1$, CTN becomes infinite.

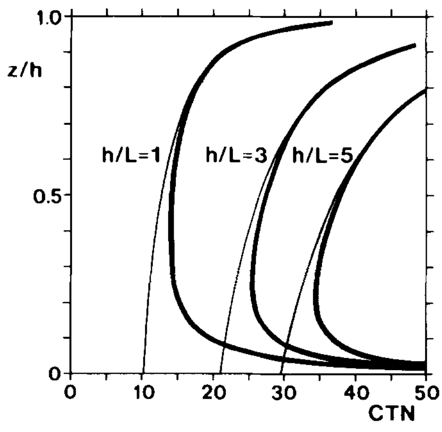

Fig. 4. Calculated profiles of the dimensionless structure parameter for different values of the stability parameter h/L. The thin lines are according to Nieuwstadt's model (10). The thick lines accord to (18) with the constants α_1 and α_2 of Nieuwstadt, i.e., $\alpha_1 = 1.5$ and $\alpha_2 = 1$.

4b. THE MODEL OF SORBJAN

In the Monin and Obukhov (1954) similarity theory of the surface layer, the non-dimensional wind shear and temperature gradients must be functions of $\zeta = z/L$ only:

$$\frac{kz}{u_*}\frac{\partial U}{\partial z} = \phi_m(\zeta)\,, \tag{11a}$$

$$\frac{kz}{T_*}\frac{\partial \Theta}{\partial z} = \phi_h(\zeta)\,. \tag{11b}$$

The theory is a great help in the analysis of the mean flow in the atmospheric boundary layer. However, similarity theory does not predict the shapes of the functions ϕ_m and ϕ_h, which can only be determined by experiments. See Yaglom (1977) for a review of the many formulas for ϕ_m and ϕ_h that have been proposed. A generally used version of the functions ϕ_m and ϕ_h is (Dyer, 1974):

$$\phi_m = \phi_h = 1 + 5\zeta\,. \tag{12}$$

Nieuwstadt (1984) introduced the idea of local scaling for the stable boundary layer. Dimensionless combinations of variables which are measured at the same height (therefore the term local is used) can be expressed as a function of a single parameter z/Λ solely, where Λ is the local Obukhov-length:

$$\Lambda = -\,\tau^{3/2}/(k\,g/T\,\overline{w'\theta'})\,. \tag{13a}$$

The local values of the Reynolds stress $\tau(z)$ and the turbulent heat flux $\overline{w'\theta'}(z)$ define the local friction velocity $U_*(z)$ and temperature scale $t_*(z)$:

$$U_*(z) = \tau^{1/2}\,, \tag{13b}$$

$$t_*(z) = -\overline{w'\theta'}/\tau^{1/2}\,. \tag{13c}$$

Nieuwstadt showed that the Cabauw observations support local scaling.

Using these local variables, one can define the following similarity functions:

$$\Phi_m = \frac{kz}{U_*}\frac{\partial \mathbf{U}}{\partial z}\,, \tag{14a}$$

$$\Phi_h = \frac{kz}{t_*}\frac{\partial \Theta}{\partial z}\,, \tag{14b}$$

$$\Phi_\epsilon = \Phi_m - Z = \frac{kz\epsilon}{U_*^3}\,, \tag{14c}$$

where $Z = z/\Lambda$. These functions must approach the Monin–Obukhov functions for $z \rightarrow 0$. Therefore, Sorbjan (1986) introduced the next hypothesis: "The form of the similarity functions Φ of Z in the outer layer (the part of the boundary layer above the surface layer) is identical to the form of Monin–Obukhov similarity functions ϕ of ζ in the surface layer". This leads to:

$$\Phi_m = \Phi_h = 1 + 5Z\,, \tag{15a}$$

$$\Phi_\epsilon = 1 + 4Z\,. \tag{15b}$$

Sorbjan assumed that the vertical profiles of stress and heat flux are given by:

$$\tau = u_*^2(1 - z/h)^{\alpha_1}\,, \tag{16a}$$

$$\overline{w'\theta'} = \overline{w'\theta'_0}(1 - z/h)^{\alpha_2}\,. \tag{16b}$$

The constants α_1 and α_2 depend *inter alia* on the state of the stable boundary layer and terrain slope and must be determined empirically. Observations give values between 1 and 2 for α_1 and values between 1 and 3 for α_2 (Lacser and Arya, 1986). One further expects that the gradients of temperature and wind speed will remain finite throughout the boundary layer. With (14), (15) and (16), this leads to the following restriction for the vertical profiles: $\alpha_2 \geqslant \alpha_1$. Because of large scatter in the data, the constants α_1 and α_2 are rather difficult to obtain for one single night. Using all his observations, Nieuwstadt (1984) found $\alpha_1 = 1.5$ and $\alpha_2 = 1$, so the restriction $\alpha_2 \geqslant \alpha_1$ was not confirmed by his data set. The fact that these values are overall means might have caused this result.

Using (13) and (16), we find the following relations between local quantities and surface quantities:

$$U_* = u_*(1 - z/h)^{\alpha_1/2}\,, \tag{17a}$$

$$t_* = T_*(1 - z/h)^{\alpha_2 - \alpha_1/2}\,, \tag{17b}$$

$$\Lambda = L(1 - z/h)^{3/2\alpha_1 - \alpha_2}\,. \tag{17c}$$

With these relations and (14), (15) and (5), we obtain the vertical profile for the structure parameter of temperature in dimensionless form:

$$\frac{C_T^2(kh)^{2/3}}{T_*^2} = 3.2\,\frac{(5\mu\, z/h + (1 - z/h)^{3/2\alpha_1 - \alpha_2})}{(4\mu\, z/h + (1 - z/h)^{3/2\alpha_1 - \alpha_2})^{1/3}} \times \frac{(1 - z/h)^{8/3\alpha_2 - 2\alpha_1}}{(z/h)^{2/3}}\,, \tag{18}$$

where $\mu = h/L$ is the stability parameter.

In Figure 4, we show by the thick lines the profiles of the dimensionless structure parameter CTN for different values of the stability parameter h/L and the constants α_1 and α_2 of Nieuwstadt. For $z/h \geqslant 0.35$, (18) gives the same results as Nieuwstadt's model, which is only valid for $z/L \gg 1$. Using this restraint and the constants of Nieuwstadt in (18), we obtain:

$$\frac{C_T^2(kh)^{2/3}}{T_*^2} \approx 3.2\,C(h/L)^{2/3}(1 - z/h)^{-1/3}\,, \tag{19}$$

where the constant $C = 5/4^{1/3} = 3.15$ equals the factor $\mathrm{Ri}/(\mathrm{Ri}_f^{5/3}(1 - \mathrm{Ri}_f)^{1/3})$ in

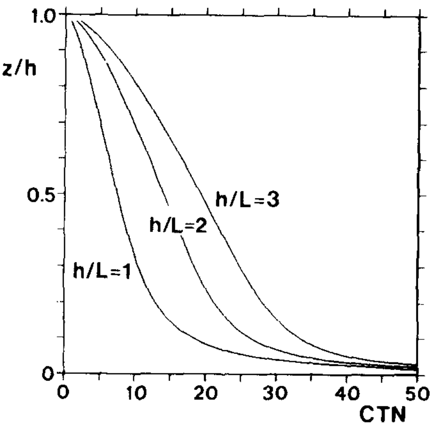

Fig. 5. The profiles of the dimensionless structure parameter using Equation (18) with $\alpha_1 = \alpha_2 = 1$ for three values of h/L.

(10) with $\mathrm{Ri} = \mathrm{Ri}_f = 0.2$. It now becomes clear that it is the closure hypothesis $\mathrm{Ri} = \mathrm{Ri}_f =$ constant that caused the structure parameter following from (10) to become constant near the surface. However, observations show that near the surface the values of Ri and Ri_f deviate from 0.2 (Figure 3). Here, by using similarity functions, the influence of the surface layer is better represented. So, we expect that the shape of the structure parameter profile in that part of the boundary layer will be better described by (18) than by Nieuwstadt's model.

We note further that CTN always increases towards the surface irrespective of $\alpha_2 > \alpha_1$ or $\alpha_2 < \alpha_1$. However, for larger z/h, the shape of the profile does depend on the value of α_2/α_1. For $\alpha_2 > \frac{3}{4}\alpha_1$, CTN $\rightarrow 0$ at the top of the boundary layer, whereas for $\alpha_2 < \frac{3}{4}\alpha_1$, the structure parameter of temperature goes to infinity. With the earlier restriction of $\alpha_2 \geq \alpha_1$, it follows that (18) describes a structure parameter decreasing with height (Figure 5), whereas, adopting Nieuwstadt's values $\alpha_1 = 1.5$ and $\alpha_2 = 1$, CTN $\rightarrow \infty$ at the top of the boundary layer (Figure 4).

4c. The Model of Duynkerke and Driedonks

To study the cloud-topped atmospheric boundary layer, Duynkerke and Driedonks (1987) developed a multilevel ensemble-averaged model. Tjemkes and Duynkerke (1989) show that this model can simulate the structure and evolution of the nocturnal boundary layer as well. In this type of model, the combined effect of all eddy sizes has to be parameterized. For this purpose, several turbulent closure hypotheses have been developed, which are mainly based on observational data from the clear-sky atmospheric boundary layer. In the model of Duynkerke and Driedonks, turbulence closure is formulated by using an equation for the turbulent kinetic energy and a diagnostic formulation for the length scale.

The ensemble-averaged equations describing the dynamics of the atmospheric boundary layer in horizontally homogeneous conditions are a more complete version of the set used by Nieuwstadt. Duynkerke and Driedonks added to these equations an equation that describes the evolution of total water, i.e., water vapor and liquid water. We adopted a low humidity in order to prevent cloud formation. Moreover, the humidity is taken independent of time and no evaporation has been considered.

The fluxes in the equations are expressed as:

$$-\overline{\phi' w'} = K_{m,h} \frac{\partial \phi}{\partial z}, \tag{20}$$

where ϕ is either a horizontal velocity component (K_m is used), or temperature or specific humidity (K_h). The exchange coefficients are calculated with:

$$K_{m,h} = c l_{m,h} E^{1/2}, \tag{21}$$

where c is a constant, $l_{m,h}$ a length scale and E the turbulent kinetic energy, determined with the complete turbulent kinetic energy budget (Businger, 1982). In the stable boundary layer, the length scale $l_{m,h}$ is determined by a suitable interpolation between two length scales; viz., a length scale for the surface layer:

$$l = kz/\phi_{m,h}, \tag{22a}$$

with $\phi_{m,h} = 1 + 5\ z/L$, and a length scale for the stable layer:

$$l_s = c_s E^{1/2}/N, \tag{22b}$$

where $c_s = 0.36$ and N is the Brunt–Väisälä frequency given by:

$$N^2 = \frac{g}{\Theta_0} \frac{\partial \Theta}{\partial z}. \tag{22c}$$

Longwave radiative cooling of the atmosphere is calculated with the band-model of Tjemkes and Duynkerke (1989), the surface temperature with a model of Deardorff (1978). For the roughness length, a value of 0.15 m is adopted, which is typical for the Cabauw surroundings. The calculations were started with a neutral temperature profile.

Two situations, with geostrophic winds of 6 and 10 m/s have been simulated. In Figure 6, the curves are shown after 4, 6, 8 and 10 hr.

With a geostrophic wind of 6 m/s, there is a continuous decrease of the structure parameter with height. The stability parameter h/L for this case is about 3. With a geostrophic wind of 10 m/s, only in the beginning of the night there is a continuous decrease of the structure parameter. After about 6 hr, the structure parameter decreases with height in the lower half of the boundary layer, while in the upper half it reaches a maximum at $z/h \approx 0.7$, decreasing again down to a small value at the top of the boundary layer. During the night, the whole curve above $z/h \approx 0.1$ moves to the right. This implies an increase of the structure parameter in the entire boundary layer, which is most pronounced

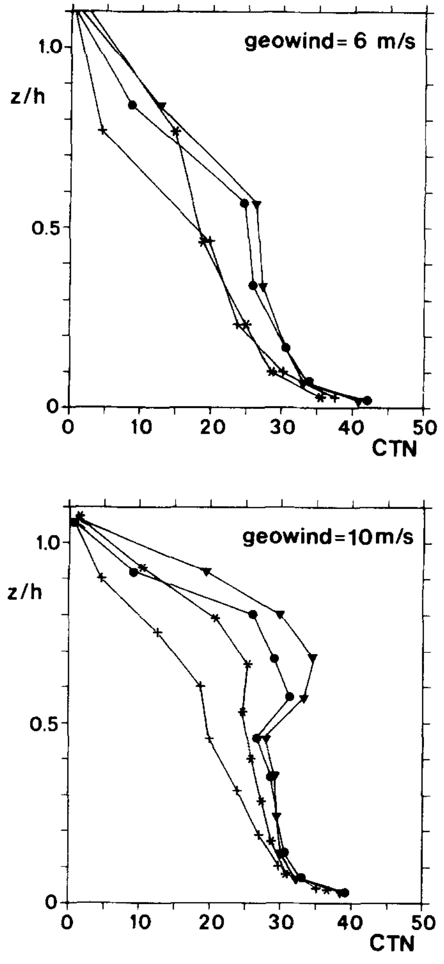

Fig. 6. Profiles of the dimensionless structure parameter calculated with the model of Duynkerke and Driedonks. Curves are shown after 4 hr (+), 6 hr (*), 8 hr (●) and 10 hr (▼), for geostrophic wind speeds of 6 and 10 m/s.

around $z/h \approx 0.6 - 0.7$. However, there is also a slight decrease of the stability parameter h/L from 2.5 to 2.0. We thus observe that CTN increases with decreasing h/L. In contrast, Nieuwstadt's model predicts an increase of the structure parameter with increasing h/L (Equation (10)). Moreover, the profiles of Nieuwstadt's model disagree with the model of Duynkerke and Driedonks. On the other hand, there is reasonable agreement between the profiles of the model of Duynkerke and Driedonks at a geostrophic wind speed of 6 m/s and the profile based on Sorbjan's hypothesis, Equation (18), with $\alpha_1 = \alpha_2 = 1$. However, the profiles with geostrophic wind $\mathbf{U}_g = 10$ m/s do not agree with (18) for any value of α_1 and α_2.

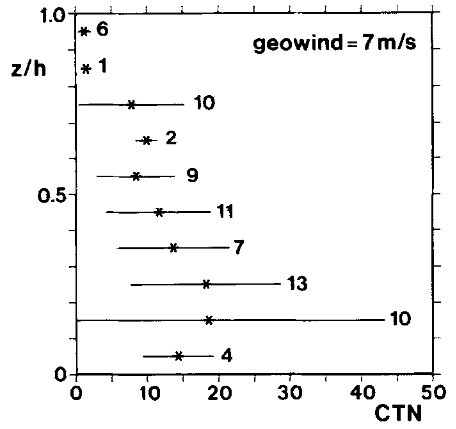

Fig. 7. Observations of the dimensionless structure parameter with data taken during the whole night for moderate geostrophic wind periods and only during the beginning of nights with a high geostrophic wind. The wind speed is the mean of the low geostrophic wind periods only. Each point indicates the average of all observations within a given height interval. The bar indicates the standard deviation of the data and the number represents the number of data points within each height interval.

5. Results and Discussion

In Figures 7 and 8, we show observations of the dimensionless structure parameter CTN for the periods mentioned in Table II. The mean geostrophic wind speed during the observation periods is indicated. From these figures it appears that the structure parameter is large near the surface and small at the top of the boundary layer. The profiles between surface layer and inversion layer can roughly be divided into two classes. First, there are observation periods when CTN decreases continuously with height. In these periods, the geostrophic wind

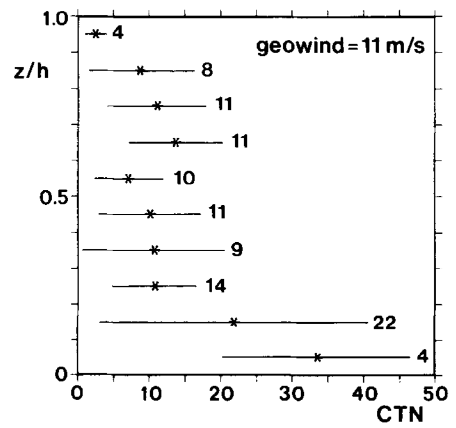

Fig. 8. As Figure 7, but for high geostrophic wind periods later at night. The mean geostrophic wind speed in these periods is indicated.

speed is about 7 m/s or there is a higher geostrophic wind speed but observations were made early at night (Figure 7). Second, in the other periods (with $\mathbf{U}_g \approx 11$ m/s and observations made later at night), CTN decreases in the lower half of the boundary layer, but shows an increase about $z/h \approx 0.7$, after which it decreases again (Figure 8).

In Figure 9, we show observations of CTN as a function of z/h where only those values of CTN were used with the stability parameter either in the interval $1.0 \leq h/L < 1.5$ or $5.5 \leq h/L < 7.0$. According to Nieuwstadt's expression (10), CTN should be about three times as large in the latter case as in the first case (Figure 4). However, the observations do not show such behaviour. The observed structure parameter does not seem to depend on the stability parameter.

In Section 4a, we concluded that according to Nieuwstadt's theory, the temperature structure parameter approaches a constant value at the surface and increases with height. The observations on the contrary show that the structure parameter increases near the surface and is small at the top of the boundary layer. The reason for the discrepancy in the surface layer is that Ri and Ri_f were assumed to be constant (0.2). Near the surface, Ri and Ri_f are smaller than 0.2 due to the high shear. At the top of the boundary layer, the assumption seems correct. The second assumption in Nieuwstadt's theory, that of stationarity, is likely to cause the theoretical profile to become infinite, which is not supported by the observations. As a consequence of this assumption, $\partial\Theta/\partial z$ is proportional to $(1 - z/h)^{-1}$. Because $\overline{w'\theta'}$ is found to be proportional to $(1 - z/h)$, the dissipation of temperature variance $N = -\overline{w'\theta'}(\partial\Theta/\partial z)$ is independent of height and consequently, the profile of CTN is determined by the profile of the dissipation of turbulent kinetic energy ϵ only (Section 4a). However, if $\partial\Theta/\partial z$ is proportional to $(1 - z/h)^{-1}$, then Θ should increase continuously with height to become infinite at the top of the boundary layer. Figure 10 shows that this does not occur. So, $\partial\Theta/\partial z$

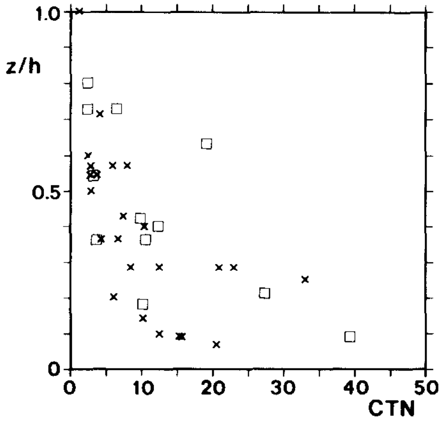

Fig. 9. Observations of the dimensionless structure parameter with the stability parameter either in the interval $1.0 \leq h/L < 1.5$ (×) or $5.5 \leq h/L < 7.0$ (□),

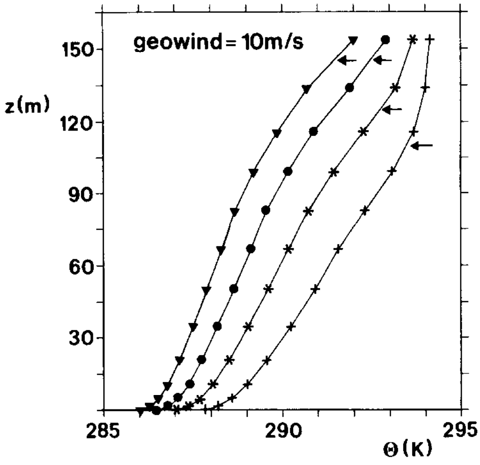

Fig. 10. Potential temperature profiles computed for two values of the geostrophic wind after 4 hr (+), 6 hr (*), 8 hr (●) and 10 hr (▼). The boundary-layer height, defined as the altitude where the heat flux is 5% of its surface value, is indicated by an arrow.

is not proportional to $(1 - z/h)^{-1}$. Therefore, N must be a function of height and the profile of CTN is determined by the profiles of ϵ and N.

Next, we turn to the model of Sorbjan. We first examine the dimensionless profiles of the temperature and wind gradient (14). Observations of these so-called similarity functions Φ_m and Φ_h are shown in Figures 11a and 11b. The line $1 + \beta z/\Lambda$ with $\beta = 5$ seems to fit reasonably well although close to the surface, β might be larger (Yaglom, 1977; Wieringa, 1980; Zhang *et al.*, 1988).

The profile of the structure parameter in the surface layer is described acceptably by using similarity functions of Sorbjan. However, above this layer the profile is sensitive to the specific values of α_1 and α_2 of the stress and heat flux profiles, Equation (16). For a single night, these values could not be determined because of large scatter in the data. But whatever choices of α_1 and α_2 are made, the profile of CTN above the surface layer either continuously increases or decreases. So, even if one were able to determine these constants, one could only expect good agreement in moderate geostrophic wind speed cases. The model can not generate the maximum of CTN observed in the upper mixed layer for the high wind speed cases. Moreover, like the model of Nieuwstadt (Section 4a), the profile of CTN is also a function of h/L. The more stable the atmosphere, the larger is CTN. As mentioned earlier, the observations do not show such behaviour (Figure 9).

The best agreement with observations is found with the profiles calculated from the model of Duynkerke and Driedonks (1987). The calculated profiles show an increase near the surface. For medium geostrophic winds (~6 m/s), there is a continuous decrease of CTN towards the top of the boundary layer.

In the situation of a strong geostrophic wind, the model shows that, after a few hours, a local maximum of CTN develops about $z/h \sim 0.7$. This behaviour can

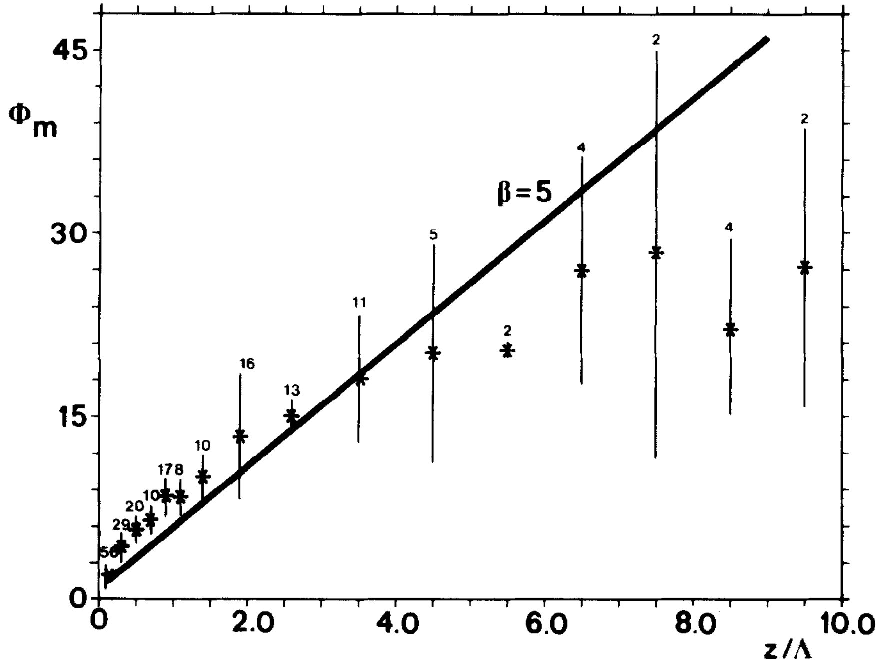

Fig. 11(a). Dimensionless profile of wind gradient Φ_m as a function of the dimensionless height z/Λ. Each point indicates the average of all observations within a given height interval. The bar indicates the standard deviation of the data and the number represents the number of data points within each height interval. Also shown is the function $\Phi = 1 + \beta z/\Lambda$ with $\beta = 5$.

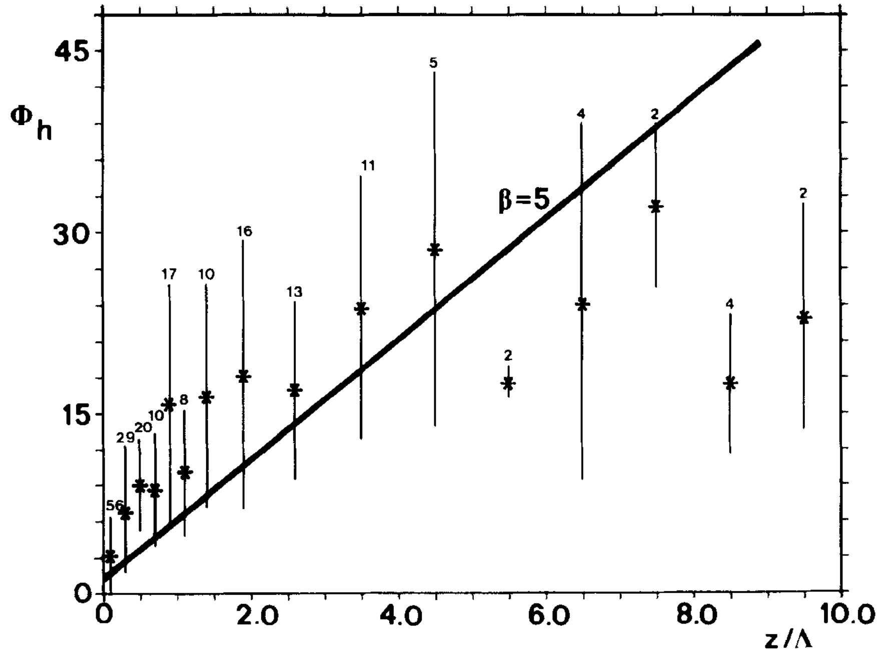

Fig. 11(b). As Figure 11(a), but for the dimensionless temperature gradient Φ_h.

roughly be understood by using the profiles of potential temperature (Figure 10). There is a large temperature gradient close to the surface. In that region, there is considerable mechanical turbulence and CTN is large. At the beginning of the night, the vertical temperature gradient decreases continuously with height and so does CTN, which depends on it. However, after a few hours, we see an increase of the temperature gradient at larger height. This causes the increase of CTN at $z/h \approx 0.7$.

So, the shapes of the calculated profiles agree qualitatively with observed profiles. The reason why the values of CTN obtained from the model are about 2–3 times as high as those observed is not clear to us. We found that adopting a value larger than 5 for β makes the discrepancy only greater.

6. Conclusions

We have examined the structure parameter of temperature in the stable, nocturnal boundary layer with continuous turbulence. The data were gathered during clear nights from the meteorological mast at Cabauw, The Netherlands.

The vertical profile of the temperature structure parameter depends on the geostrophic wind speed. On nights with a moderate geostrophic wind speed and in the first few hours of nights with a high geostrophic wind speed, the structure parameter is large near the surface and decreases continuously to become small at the top of the boundary layer. On nights with a high geostrophic wind speed, the observations show, a few hours after transition, the development of a maximum of the structure parameter at about three quarters of the boundary-layer height.

Comparing these observations with three theoretical profiles leads to the following conclusions:

Because of the assumptions of stationarity and constant Ri and Ri_f, the model of Nieuwstadt (1985) is not suited to describe the profile of the structure parameter.

Using similarity functions following Sorbjan (1986), we found qualitative agreement between observations and model in the lower part of the boundary layer. Because the constants α_1 and α_2 in the stress and heat flux profiles could not be determined experimentally separately for each night, we can not simulate the profiles in the rest of the boundary layer. However, calculations with assumed values of α_1 and α_2 show that the maximum at $z/h \approx 0.7$ observed on nights with a high geostrophic wind can not be explained. Like the model of Nieuwstadt, the model using similarity functions shows that the profile of CTN is a function of the stability parameter. The observations do not show such a dependency.

The model of Duynkerke and Driedonks shows the right shape of the profile in moderate and high geostrophic wind speed situations. However, the computed value of the structure parameter is 2–3 times higher than observed.

Acknowledgements

The authors wish to thank Dr P. G. Duynkerke for calculating the profiles of the temperature structure parameter. We thank him and Dr A. P. van Ulden for useful comments on earlier versions of the manuscript.

References

Brost, R. A. and Wyngaard, J. C.: 1978, 'A Model Study of the Stably Stratified Planetary Boundary Layer', *J. Atmos. Sci.* **35**, 1427–1440.

Businger, J. A.: 1982, 'Equations and Concepts', in F. T. M. Nieuwstadt and H. van Dop (eds.), *Atmospheric Turbulence and Air Pollution Modelling*, D. Reidel Publ. Co., pp. 1–36.

Caughey, S. J., Wyngaard, J. C., and Kaimal, J. C.: 1979, 'Turbulence in the Evolving Stable Boundary Layer', *J. Atmos. Sci.* **36**, 1041–1052.

Champagne, F. H., Friehe, C. A., LaRue, J. C., and Wyngaard, J. C.: 1977, 'Flux Measurements, Flux Estimation Techniques, and Fine-Scale Turbulence Measurements in the Unstable Surface Layer Over Land", *J. Atmos. Sci.* **34**, 515–530.

Corrsin, S.: 1951, 'On the Spectrum of Isotropic Temperature Fluctuations in an Isotropic Turbulence', *J. Appl. Phys.* **22**, 469–473.

Coulman, C. E.: 1985, 'Fundamental and Applied Aspects of Astronomical Seeing', *Ann. Rev. Astron. Astrophys.* **23**, 19–57.

Coulter, R. L. and Wesely, M. L.: 1980, 'Estimates of Surface Heat Flux From Sodar and Laser Scintillation Measurements in the Unstable Boundary Layer', *J. Appl. Meteorol.* **19**, 1209–1222.

Deardorff, J. W.: 1978, 'Efficient Prediction of Ground Surface Temperature and Moisture, with Inclusion of a Layer of Vegetation', *J. Geophys. Res.* **83**, 1889–1903.

Driedonks, A. G. M. and de Baas, A. F.: 1983, 'Internal Waves in the Stably Stratified Atmospheric Boundary Layer', Preprints Sixth Symp. on Turbulence and Diffusion, Boston, Amer. Meteorol. Soc., 276–279.

Duynkerke, P. G. and Driedonks, A. G. M.: 1987, 'A Model for the Turbulent Structure of the Stratocumulus-Topped Atmospheric Boundary Layer', *J. Atmos. Sci.* **44**, 43–64.

Dyer, A. J.: 1974, 'A Review of Flux-Profile Relationships', *Boundary-Layer Meteorol.* **7**, 363–372.

Fairall, C. W.: 1987, 'A Top-Down and Bottom-up Diffusion Model of C_T^2 and C_Q^2 in the Entraining Convective Boundary Layer', *J. Atmos. Sci.* **44**, 1009–1017.

Finnigan, J. J. and Einaudi, F.: 1981, 'The Interaction Between an Internal Gravity Wave and the Planetary Boundary Layer, Part II: Effect of the Wave on the Turbulence Structure', *Quart. J. Roy. Meteorol. Soc.* **107**, 807–832.

Garratt, J. R. and Brost, R. A.: 1981, 'Radiative Cooling Effects within and Above the Nocturnal Boundary Layer', *J. Atmos. Sci.* **38**, 2730–2746.

Herben, M. H. A. J.: 1983, 'Amplitude Scintillations on the OTS-TM/$\overline{\text{TM}}$ Beacon', *Archiv für Elektronik und Übertragungstechnik* **37**, 130–132.

Hill, R. J. and Ochs, G. R.: 1983, 'Surface-Layer Micrometeorology by Optical Scintillation Techniques', *Remote Probing of the Atmosphere*, Technical Digest of the Topical Meeting on Optical Techniques for Remote Probing of the Atmosphere, Washington, D.C., Optical Society of America, TuC16.1–TuC16.4.

Hinze, J. O.: 1975, *Turbulence*, McGraw-Hill, New York.

Kondo, J., Kanechika, O., and Yasuda, N.: 1978, 'Heat and Momentum Transfer and Strong Stability in the Atmospheric Surface Layer, *J. Atmos. Sci.* **35**, 1012–1021.

Lacser, A. and Arya, S. P. S.: 1986, 'A Numerical Model Study of the Structure and Similarity Scaling of the Nocturnal Boundary Layer', *Boundary-Layer Meteorol.* **35**, 369–385.

Monin, A. S. and Obukhov, A. M.: 1954, 'Basic Laws of Turbulent Mixing in the Atmosphere Near the Ground', *Tr. Geophys. Inst. Ak. Nauk SSSR* **24**, 163–187.

Monna, W. A. A. and van der Vliet, J. G.: 1987, 'Facilities for Research and Weather Observations on the 213 m Tower at Cabauw and at Remote Locations', Scientific Reports WR-nr 87-5, KNMI, De Bilt, The Netherlands.

Nieuwstadt, F. T. M.: 1984, 'The Turbulent Structure of the Stable, Nocturnal Boundary Layer', *J. Atmos. Sci.* **41**, 2202–2216.

Nieuwstadt, F. T. M.: 1985, 'A Model for the Stationary, Stable Boundary Layer', in J. C. R. Hunt (ed.), *Turbulence and Diffusion in Stable Environments*, Clarendon Press, Oxford, England, 149–179.

Ochs, G. R. and Hill, R. J.: 1985, 'Optical-Scintillation Method of Measuring Inner Scale', *Appl. Opt.* **24**, 2430–2432.

Sorbjan, Z.: 1986, 'On Similarity in the Atmospheric Boundary Layer', *Boundary-Layer Meteorol.* **34**, 377–397.

Tatarski, V. I.: 1961, *Wave Propagation in a Turbulent Medium* (translated by R. A. Silverman), McGraw-Hill, New York.

Tjemkes, S. A. and Duynkerke, P. G.: 1989, 'The Nocturnal Boundary Layer. Model Calculations Compared with Observations', *J. Appl. Meteorol.* (to be published).

Wieringa, J.: 1967, 'Evaluation and Design of Windvanes', *J. Appl. Meteorol.* **6**, 1114–1122.

Wieringa, J.: 1972, 'Tilt Errors and Precipitation Effects in Trivane Measurements of Turbulent Fluxes over Water', *Boundary-Layer Meteorol.* **2**, 406–426.

Wieringa, J.: 1980, 'A Revaluation of the Kansas Mast Influence on Measurements of Stress and Cup Anemometer Overspeeding', *Boundary-Layer Meteorol.* **18**, 411–430.

Wyngaard, J. C. and LeMone, M. A.: 1980, 'Behaviour of the Refractive Index Structure Parameter in the Entraining Convective Boundary Layer', *J. Atmos. Sci.* **37**, 1573–1585.

Yaglom, A. M.: 1977, 'Comments on Wind and Temperature Flux-Profile Relationships', *Boundary-Layer Meteorol.* **11**, 89–102.

Zhang, S. F., Oncley, S. P., and Businger, J. A.: 1988, 'A Critical Evaluation of the von Karman Constant from a New Atmospheric Surface Layer Experiment', Preprints Eighth Symp. on Turbulence and Diffusion, San Diego, Amer. Meteorol. Soc., 148–150.